ELSEVIER

Biophysical Chemistry 110 (2004) 297–308

Biophysical Chemistry

www.elsevier.com/locate/bpc

Voltammetric studies of hemoglobin-coated polystyrene latex bead films on pyrolytic graphite electrodes

Hong Sun[a,b], Naifei Hu[a,*]

[a] *Department of Chemistry, Beijing Normal University, 19 Xinjiekouwai Street, Beijing 100875, China*
[b] *School of Chemical Engineering, Qingdao University, Qingdao 266071, China*

Received 24 November 2003; received in revised form 1 March 2004; accepted 5 March 2004
Available online 21 April 2004

Abstract

A novel hemoglobin (Hb)-coated polystyrene (PS) latex bead film was deposited on pyrolytic graphite (PG) electrode surface. In the first step, positively charged Hb molecules in pH 5.0 buffers were adsorbed on the surface of negatively charged, 500 nm diameter PS latex beads bearing sulfate groups by electrostatic interaction. The aqueous dispersion of Hb-coated PS particles was then deposited on the surface of PG electrodes and, after evaporation of the solvent, Hb-PS films were formed. The Hb-PS film electrodes exhibited a pair of well-defined, quasi-reversible cyclic voltammetric (CV) peaks at about −0.36 V vs. SCE in pH 7.0 buffers, characteristic of Hb heme Fe(III)/Fe(II) redox couples. Positions of Soret absorption band of Hb-PS films suggest that Hb retains its near-native structure in the films in its dry form and in solution at medium pH. The Hb in PS films was also acted as a catalyst to catalyze electrochemical reduction of various substrates such as trichloroacetic acid (TCA), nitrite, oxygen and hydrogen peroxide.

Keywords: Hemoglobin; Polystyrene latex bead; Film modified electrode; Direct electrochemistry; Electrocatalysis

1. Introduction

Thin protein films have attracted a great interest among researchers because of their broad application in biotechnology such as biosensing, bioseparation, immunoassay, diagnostics and catalysis [1–3]. In recent years, redox protein films modified on electrode surface have been developed to achieve direct electron transfer of proteins with underlying electrodes [4,5]. Direct electrochemistry of redox proteins or enzymes may provide a working model for the mechanistic study of electron transfer between enzymes in biological systems, and serve as a basis for fabricating new kinds of electrochemical biosensors, enzymatic bioreactors and biomedical devices by removing the requirement of chemical mediators [6–8].

Our long-term goal is to develop various supporting films on electrode surface to immobilize redox proteins or enzymes. The proteins incorporated in the films on electrodes should exhibit well-defined and direct electrochemical responses, retain their native properties and enzymatic activities, and demonstrate a good stability. Successful

* Corresponding author. Tel.: +81-10622-7838; fax: +81-10622-02075.
E-mail address: hunaifei@bnu.edu.cn (N. Hu).

0301-4622/$ - see front matter © 2004 Elsevier B.V. All rights reserved.
doi:10.1016/j.bpc.2004.03.005

examples have included cast films of proteins with insoluble surfactants [9,10], hydrogel polymers [11–13], biopolymers [14,15], nanoparticles [16,17], polyelectrolyte- [18,19] or clay-surfactant [20] composites, and films of proteins and polyions [21,22] or clay nanoparticles [23,24] grown layer by layer. These films facilitated direct, reversible electron transfer between the proteins and electrodes compared to that on bare electrodes with the proteins in solution.

Recently, the protein films assembled on planar solid supports has been extended to submicrometer-sized spherical latex particles or colloids by Caruso and Mohwald [25], Caruso and Schuler [26], Lvov and Caruso [27] and Schuler and Caruso [28]. In this process, for example, charged proteins at appropriate pH in solution was adsorbed in alteration with oppositely charged polyelectrolytes on the surface of polystyrene (PS) latex beads, forming a monolayer or multilayer protein shell. This organized protein shell on colloid particles demonstrated better catalytic activity and stability, and showed a promising applicability as a new class of bioreactors [25–28].

Stimulated and aroused by the works of Caruso et al., we are now trying to construct the redox protein shell on the surface of colloid particles, and then assemble the protein-coated particles onto electrode surface. We expect that the proteins in this new kind of films would exhibit good direct electrochemistry and electrocatalytic properties, and retain their native structure. The present work is our first attempt in this direction. In this report, positively charged hemoglobin (Hb) at pH 5.0 was first adsorbed on the surface of 500 nm diameter PS latex particles carrying negatively charged groups on their surface through electrostatic interaction, and the aqueous dispersion of Hb-coated PS latex particles was then deposited on the surface of pyrolytic graphite (PG) electrodes. These unique PS particle films provided a favorable microenvironment for Hb, and enhanced the direct, reversible electron transfer between Hb and underlying PG electrodes. Electrochemical catalytic reductions of various substrates of environmental or biological significance were also observed at Hb-PS film electrodes, indicating the potential applicability of the films as biosensors or bioreactors.

2. Experimental

2.1. Reagents

Bovine hemoglobin (Hb, MW 66,000, 90%) was from Shanghai Lizhu Dongfeng Biotechnology and used as received without further purification. Polystyrene latex beads (diameter 500 nm) bearing negatively charged sulfate groups on their surface supplied as an aqueous suspension (solid contents 2.5%) were purchased from Sigma. Trichloroacetic acid (TCA) was from Beijing Dongjiao Chemicals; sodium nitrite was from Beijing Sanhuan Chemicals; and hydrogen peroxide (H_2O_2, 30%) was from Beijing Chemical Engineering Plant. All other chemicals were of analytical grade. The supporting electrolyte was usually 0.05 M potassium dihydrogen phosphate buffers at pH 7.0 containing 0.1 M KBr. Other buffers were 0.1 M sodium acetate, 0.1 M boric acid or 0.1 M citric acid, all containing 0.1 M KBr. The pHs of buffers were regulated with HCl or NaOH solutions. Solutions were prepared with twice distilled water.

2.2. Assembly of Hb on PS latex particles

A total of 2.5 μl of 2.5% PS aqueous suspension (about 10^9 PS particles) was added to a centrifuge tube containing 1 ml of 1 mg ml^{-1} Hb in pH 5.0 buffers. With the isoelectric point at pH 7.4 [29], Hb was positively charged at pH 5.0 and would adsorb on the surface of negatively charged PS latex particles by electrostatic attraction. The dispersion was kept at 4 °C for 4 h with occasional stir so that the adsorption equilibrium of Hb on PS beads was obtained. The dispersion was then centrifuged at 10,000 rpm for 6 min to separate the beads with the supernatant. The supernatant containing the unadsorbed Hb was discarded. In the next washing step, 1 ml of pure water was added into the tube and mixed with the Hb-coated PS latex beads, designated as Hb-PS. After the Hb-PS particles were redispersed in water by gentle shaking, centrifugation was performed again and the supernatant was discarded. This redispersion/centrifugation/discarding cycle was repeated two additional times to ensure removal of all free or unadsorbed Hb from the PS particles. After being washed thoroughly, the Hb-PS beads were dispersed in 200 μl of pH 5.0 buffers and the dispersion was stored in refrigerator at 4 °C.

2.3. Deposition of Hb-PS films on electrodes

Prior to use, basal plane PG (Advanced Ceramics, geometric area 0.16 cm^2) disk electrodes were polished with metallographic sandpapers of 1200 grit while being flushed with water. Electrodes were then ultrasonicated in pure water for 30 s. Typically, 8 μl of the prepared Hb-PS dispersions were cast onto a freshly polished PG electrode. A small bottle was fit tightly over the electrode to serve as a closed evaporation chamber for several hours so that the water was evaporated slowly and more uniform films were formed. The Hb-PS films were then dried in air overnight.

2.4. Instrumentation and procedure

UV–vis absorption spectroscopic measurements of Hb-PS films on quartz slides were performed with a Cintra 10e UV–visible spectrophotometer (GBC). Prior to use, the quartz slides were pretreated by ultrasonication in a washing solution (1% KOH+ 49% ethanol+50% water) for 15 min, and then carefully rinsed with water. Hb-PS films were prepared by depositing the dispersion of Hb-PS particles onto the slides and then being dried overnight in air.

Cyclic voltammetry (CV) and square wave voltammetry (SWV) were performed using a CHI 660A electrochemical workstation (CH Instruments). A three-electrode cell was used where a PG disk coated with Hb-PS films acted as working electrode, a platinum flake as counter electrode, and a saturated calomel electrode (SCE) as reference electrode. Voltammetries of Hb-PS films were performed in buffers containing no Hb. Buffers were purged with highly purified nitrogen for about 20 min before a series of experiments. A nitrogen environment was then maintained in the cell by continuously bubbling N_2 during the whole experiment. In the CV experiments with O_2, measured volumes of air were injected through solution via a syringe in a sealed cell, which had been previously degassed with purified nitrogen. All experiments were performed at room temperature of 18±2 °C. The Hb-PS film electrodes were stored in the refrigerator at 4 °C when they were not used.

Electrophoretic mobility of bare PS latex beads and Hb coated PS particles was measured in water with a Nicomp 380/ZLS zeta-potential analyzer (Particle Sizing Systems). The electrophoretic mobility (u) of charged particles was determined by measuring the Doppler shift in frequency of light scattered from the moving particles in an applied electric field. The zeta-potential (ζ) was then calculated from the electrophoretic mobility by using the Smoluchowski relation $\zeta=u\eta/\varepsilon$, where η and ε are the viscosity and permittivity of the solution, respectively.

3. Results and discussion

3.1. Adsorption of Hb on PS latex particles

The adsorption of Hb on PS latex beads was confirmed by zeta-potential or electrophoretic mobility measurements. The negatively charged PS particles showed a zeta-potential at −20.3 mV in water. When the positively charged Hb was adsorbed on the PS surface, the zeta-potential increased to about −10.0 mV. Ideally, when positively charged Hb is the outermost layer, a positive zeta-potential would be expected. However, the measured zeta-potential of Hb-PS beads was negative. The reason for this is not very clear yet, but the similar situation was observed for the HRP/PSS (horseradish peroxidase/poly(styrenesulfonate)) system when the $(HRP/PSS)_n$ films were layer-by-layer assembled on PS particle surface [26]. Nevertheless, the positive shift of the zeta-potential is a qualitative evidence for the adsorption of Hb on PS surface.

The adsorption of Hb on PS latex particles was also followed indirectly by UV–vis spectroscopy. The Soret absorption band of Hb at 406 nm was measured for the initial (standard) Hb solution at pH 5.0 before the PS particles were added (Fig. 1a). After the addition of PS beads into the Hb solution and the completion of adsorption, the Soret band was measured again for the supernatant (Fig. 1b). In a series of washing steps with the same volume of water, UV–vis spectroscopic measurements were also conducted for the supernatants (Fig. 1c–e). The results showed that, after three cycles of redispersion/centrifugation/discarding steps, the amount of free or unadsorbed Hb in the supernatant was very limited and could not even be detected (Fig. 1e). The amount of adsorbed Hb on the PS latex particle surface was then determined by subtracting the absorbance at 406 nm of the super-

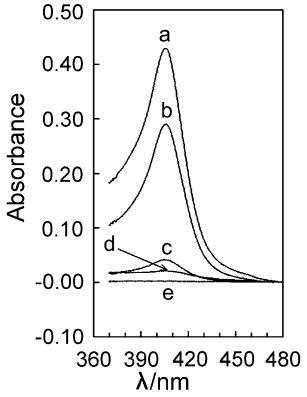

Fig. 1. UV–vis absorption spectra of (a) initial Hb solution, (b) supernatant after adsorption equilibrium of Hb on PS beads was reached, (c) supernatant after the first time of washing, (d) supernatant after the second time of washing and (e) supernatant after the third time of washing. Each solution has volume of 1 ml, respectively.

natants (Fig. 1b–d) from that of the initial Hb solution (Fig. 1a). From the difference in these spectra, it was estimated that about 10% of the total Hb in solution were adsorbed on the PS spheres. The color of PS beads became light red after adsorption of Hb, which was observed by naked eyes, also indicating the formation of Hb layer on the PS latex particle surface. These results suggest that the electrostatic attraction between positively charged Hb at pH 5.0 and negatively charged PS particles is quite strong, and the adsorption of Hb on PS particle surface is very stable, since the adsorbed Hb on the PS particle surface can withstand several cycles of water washing.

3.2. Conformational studies

The Soret absorption band of heme proteins may provide information on the protein denaturation, and it is especially sensitive to the conformational change in the heme region [30,31]. UV–visible spectroscopy was therefore used to observe the position change of Soret band for Hb-PS films. Both dry Hb-PS and Hb films cast on quartz slides showed Soret band at 412 nm (Fig. 2a,b), suggesting that Hb adsorbed on the surface of PS latex particles has a structure nearly the same as the native state of Hb. When the films were immersed into buffer solutions at pH between 5.0 and 10.0, the Soret band also appeared at 412 nm (Fig. 2d–f), the same as that of dry Hb and Hb-PS films, indicating that Hb coated on PS latex particles essentially retain its native state in buffers at medium pH. When pH was changed toward more acidic or more basic direction, the Soret band showed a blue-shift and some distortion. At pH 3.0, for example, the peak shifted to about 390 nm and became shape-distorted (Fig. 2g), suggesting considerable denaturation of Hb in PS films at this relatively acidic pH.

3.3. Cyclic voltammetry of Hb-PS films

When Hb-PS film electrodes were placed into pH 7.0 buffers free of Hb, after several CV scans, a pair of well-defined, quasi-reversible CV peaks at about −0.36 V vs. SCE was observed (Fig. 3b). The peak pair was attributed to the heme Fe(III)/Fe(II) redox couples of Hb [32]. PS films alone coated on a PG electrode showed no CV peak in the same potential range (Fig. 3a). The results indicate that at least parts of Hb in Hb-PS films display electroactivity when immobilized on the electrodes. In contrast, Hb in buffers at pH 7.0 showed no CV peaks in the same potential window at bare PG electrodes. Thus, the PS latex particle films cast on electrodes must have a great effect on the Hb electron transfer kinetics and provide a favorable microenvironment for Hb to transfer electrons with underlying PG electrodes, while the exact nature of this effect is not yet very

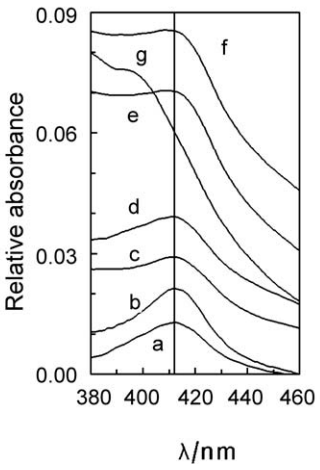

Fig. 2. UV–vis absorption spectra of films on quartz for (a) dry Hb-PS films, (b) dry Hb films and Hb-PS films in different pH buffer solutions: (c) pH 5.0, (d) pH 7.0, (e) pH 9.0, (f) pH 10.0, (g) pH 3.0.

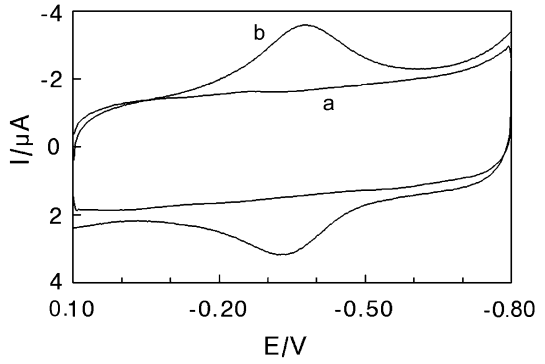

Fig. 3. Cyclic voltammograms at scan rate of 0.2 V s^{-1} in pH 7.0 buffer solutions containing no Hb for (a) PS latex particles films and (b) Hb-PS films at the steady state.

clear. One possibility is that in the assembly of Hb on PS sphere surface, several cycles of washing/discarding steps may remove the macromolecular impurities originally existing in Hb solution. Otherwise, the impurities could adsorb on electrode surface and block the electron transfer of the proteins in solution at bare electrodes [33]. The good selectivity of PS beads toward Hb adsorption rather than the impurities, combined with the washing/removing steps, may make the assembly procedure act as a purification process.

CVs of Hb-PS films had a nearly symmetric peak shape and approximately equal heights of reduction and oxidation peaks. The reduction peak current increased linearly with scan rate from 0.05 to 2 V s^{-1}. Integration of reduction peak at different scan rate gave nearly constant charge (Q) values. All these are characteristic of quasi-reversible, diffusionless or thin-layer electrochemistry [34]. The surface concentration of electroactive Hb in the films (Γ^*) was estimated to be 2.65×10^{-11} mol cm^{-2} according to the relationship of $Q=nAF\Gamma^*$ [34], where n is the number of electrons transferred for each Hb molecule (4), A is the electrode area (0.16 cm^2), F is Faraday's constant. Based on the Hb concentration we used (1 mg ml^{-1}), the fraction of Hb loaded on PS (10%) and the relative amount of Hb-PS beads cast on electrodes (8 μl/200 μl), the surface concentration of the total amount of Hb deposited on the electrode surface was estimated to be 3.81×10^{-10} mol cm^{-2}. Thus, the fraction of electroactive Hb among the total Hb deposited would be about 7%. The reason why the fraction value is relatively very low is not clear yet and needs to be further investigated. It may suggest rather aggregates of Hb on PS beads, and the aggregation of Hb may hinder the electroactivity of Hb. Nevertheless, when the same amount of Hb (3.8×10^{-10} mol cm^{-2}) was directly cast on PG electrodes, the CV response under the same condition was much smaller than that for Hb-PS films, indicating a larger extent of aggregation of Hb on PG surface and an even smaller electroactivity fraction.

An increase in buffer pH caused a negative shift in potentials of both CV reduction and oxidation peaks for Hb-PS films. In general, all changes in CV peak potentials and currents with pH were reversible between pH 5.0 and 11.0. For example, CVs for an Hb-PS film in a pH 7.0 buffer were reproducible after immersing the film in a pH 10.0 buffer and then returning it to the pH 7.0 buffer. CV data were used to investigate the pH effect on the formal potential ($E^{\circ\prime}$), which was estimated as the midpoint of reduction and oxidation peak potentials. $E^{\circ\prime}$ had a linear relationship with pH between pH 5.0 and 12.0 with a slope of −54 mV pH^{-1} (Fig. 4). This slope value was reasonably close to the theoretical value of −57.7 mV pH^{-1} at 18 °C for a reversible electron transfer coupled to proton transportation with equal number of protons and electrons [35], which could be represented by

$$\mathrm{HbhemeFe(III)} + \mathrm{H^+} + \mathrm{e^-} \rightleftharpoons \mathrm{HbhemeFe(II)}$$

An inflection point appeared at pH 5.0 in the $E^{\circ\prime}$–pH plot. Below pH 5.0, $E^{\circ\prime}$ varied with pH with a much smaller slope (Fig. 4). The position of the break

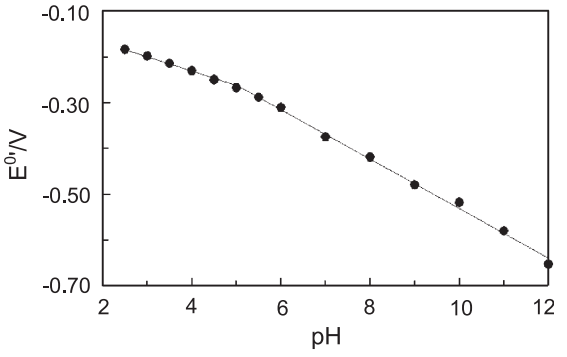

Fig. 4. Influence of pH on formal potentials ($E^{\circ\prime}$) estimated as an average of CV reduction and oxidation peak potentials for Hb-PS films at 0.2 V s^{-1}.

in the $E^{\circ\prime}$ –pH plot suggests that the protonated site associated with electrode reaction has an apparent pK_a value of 5.0 [9,36,37].

Long-term stability is one of the most important features required for a biosensor. The stability of Hb-PS films was examined by CV under two different conditions. In the solution study, a PG electrode coated with Hb-PS films was stored in pH 7.0 buffers all the time and CVs were run periodically. Alternatively, an Hb-PS film electrode was stored in air as its dry form for most of the storage time and CVs were run occasionally after placing the dry electrode in the buffers. With both methods, the Hb-PS films showed excellent stability. For example, after 3 weeks of storage in buffers, the Hb-PS film electrode exhibited no changes in CV peak potentials and a less than 10% decrease in reduction peak height compared with the initial steady state value.

3.4. Estimation of electrochemical parameters

SWV combined with nonlinear regression analysis was used to estimate the apparent heterogeneous electron transfer rate constant (k_s) and formal potential ($E^{\circ\prime}$) for the Hb-PS films. The theoretical model used here was a combination of a surface-confined or diffusionless SWV model [38] with a formal potential dispersion model, as described in detail previously [9,39]. The procedure employed nonlinear regression analysis for background subtracted SWV forward and reverse curves with a $5-E^{\circ\prime}$ dispersion model, as in other protein film systems [5,39]. The analysis of SWV data for Hb-PS films showed accuracy of fit of the model over a range of amplitudes and frequencies. Some examples are showed in Fig. 5. The average k_s and $E^{\circ\prime}$ values for Hb-PS films at pH 7.0 were estimated to be 58 s^{-1} and −0.35 V, respectively. The electrochemical parameters for other Hb film systems are also listed in Table 1 for comparison.

Considering the estimation error, the k_s value of Hb-PS films was close to that of other Hb films and all of them were in the same order of magnitude. Good agreement of the formal potential values was obtained between SWV and CV methods for the same Hb-PS films. However, the $E^{\circ\prime}$ value of heme Fe(III)/Fe(II) redox couples for Hb-PS films was different from that for other Hb films (Table 1). This confirms a specific effect of the film environment on $E^{\circ\prime}$ of heme proteins that has been reported previously [9,40]. Film components may shift the formal potential through interaction with protein or by their influence on the electrode double-layer. Different film components may provide different microenvironments for the same protein and influence its formal potential [9].

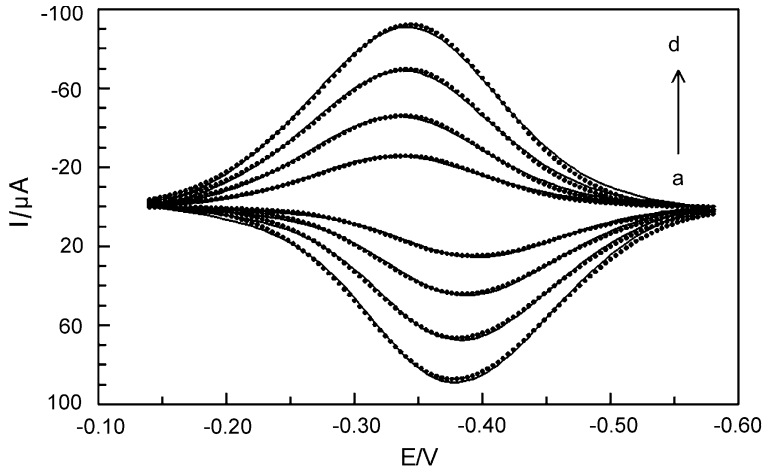

Fig. 5. Square wave forward and reverse current voltammograms for Hb-PS films in pH 7.0 buffer solutions at different frequencies. Points represent the experimental SWV from which background has been subtracted. The solid lines are the best fit by nonlinear regression onto the $5-E^{\circ\prime}$ dispersion model. SWV conditions: pulse height 60 mV, step height 4 mV and frequencies (Hz): (a) 100, (b) 132, (c) 161, (d) 192.

Table 1
Apparent heterogeneous electron transfer rate constants (k_s) and formal potentials ($E^{\circ\prime}$) for hemoglobin films on PG electrodes in pH 7.0 buffers containing no Hb

Films[a]	k_s (s^{-1})	$E^{\circ\prime}/V$ (vs. SCE)		Reference
		CV	SWV	
Hb-PS	58±6	−0.360	−0.350	This work[b]
Hb-DMPC	70±9	−0.329	−0.331	[10]
Hb-PAM	45±8	−0.320	−0.312	[12]
Hb-gluten	67±8	−0.334	−0.338	[15]
Hb-CS	104±34	−0.337	−0.344	[14]
Hb-clay	31±2	−0.347	−0.360	[16]
Hb-DDAB-PSS	33±5	−0.220	−0.204	[18]
Hb-DDAB-clay	75±8	−0.309	−0.308	[20]

[a] DMPC=dimyristoyl phosphatidylcholine, PAM=polyacrylamide, CS=chitosan, DDAB=didodecyldimethylammonium bromide, PSS=poly(styrene sulfonate).

[b] Average values for analysis of eight SWVs at frequencies of 100–200 Hz, amplitudes of 60–75 mV and a step height of 4 mV.

3.5. Catalytic reduction of TCA and $NaNO_2$

Electrocatalytic reactivity of Hb-PS films toward various substrates was investigated. When TCA was added to a pH 5.5 buffer, Hb-PS films showed an increase in the reduction peak at about −0.4 V (Fig. 6d) compared with that in the absence of TCA (Fig. 6c). The increase of HbFe(III) reduction peak was accompanied by the decrease of HbFe(II) oxidation peak, since HbFe(II) had reacted with TCA. The reduction peak current increased with the concentration of TCA in solution (Fig. 6e). The direct reduction of TCA at blank PS film electrodes was observed at a potential of more negative than −1.0 V (Fig. 6b). Thus, the reduction overpotential of TCA was decreased by at least 0.6 V. These results are characteristic of electrochemical catalysis, where HbFe(II), the reduction product of the electrode reaction, was oxidized by TCA in a chemical reaction and returned to HbFe(III) form, forming a catalytic cycle. In the previous work with myoglobin-didodecyldimethylammonium bromide (Mb-DDAB) film electrodes [41], TCA presumably underwent stepwise reductive dechlorination to ultimately become acetic acid. We speculate that the catalytic reduction of TCA on Hb-PS films would take the similar mechanism.

The catalytic reduction of nitrite with Hb-PS films was also investigated by CV. When NO_2^- was added to a pH 5.5 buffer, a new reduction wave at about −0.75 V was observed, while the Hb Fe(III)/Fe(II) peak pair was nearly intact (Fig. 7d). The new reduction peak current increased with the concentration of nitrite in solution (Fig. 7e). The direct reduction of nitrite at blank PS film electrodes was observed at the potential of more negative than −1.2 V (Fig. 7b). Thus, the reduction overpotential of nitrite was decreased by at least 0.4 V. All these

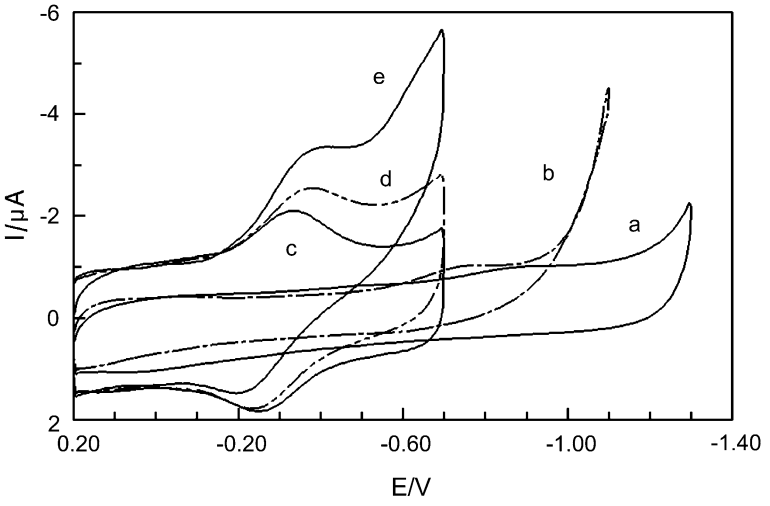

Fig. 6. Cyclic voltammograms at 0.2 V s^{-1} in pH 5.5 buffer solutions for (a) PS films with no TCA present, (b) PS films with 0.05 mM TCA present, (c) Hb-PS films with no TCA present, (d) Hb-PS films with 0.02 mM TCA present and (d) Hb-PS films with 0.05 mM TCA present.

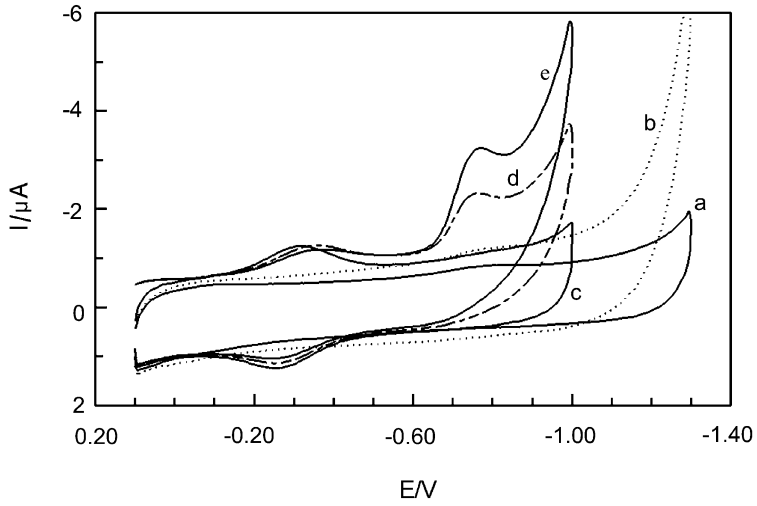

Fig. 7. Cyclic voltammograms at 0.1 V s^{-1} in pH 5.5 buffers for (a) PS films with no $NaNO_2$ present, (b) PS films with 5 mM $NaNO_2$ present, (c) Hb-PS films with no $NaNO_2$ present, (d) Hb-PS films with 5 mM $NaNO_2$ present, (e) Hb-PS films with 10 mM $NaNO_2$ present.

are characteristic of catalytic reduction of NO_2^-. Similar behavior of electrocatalytic reduction of nitrite was also observed in other Hb films [14,22]. For Hb-PS films, the catalytic CV reduction peak of nitrite had a linear relationship with NO_2^- concentration in the range of 6–16 mM with a detection limit of 1 mM and a correlation coefficient of 0.999.

3.6. Catalytic reactivity toward O_2 and H_2O_2

Electrocatalytic reduction of dioxygen in solution by Hb-PS films was examined by CV (Fig. 8). When a certain volume of air was passed through a pH 7.0 buffer by a syringe, a significant increase in reduction peak at about −0.4 V was observed for Hb-PS films (Fig. 8d). This increase in HbFe(III) reduction

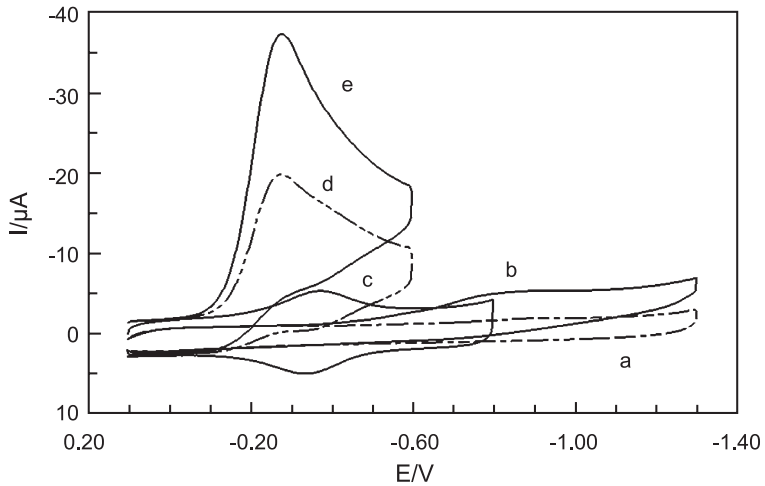

Fig. 8. Cyclic voltammograms at 0.2 V s^{-1} in 10 ml of pH 7.0 buffers for (a) PS films with no oxygen present, (b) PS films after 30 ml of air was injected into a sealed cell, (c) Hb-PS films with no oxygen present, (d) Hb-PS films after 30 ml of air was injected and (e) Hb-PS films after 60 ml of air was injected.

peak was accompanied by the disappearance of HbFe(II) oxidation peak, because HbFe(II) had reacted with oxygen. An increase in the amount of oxygen in solution increased the reduction peak current (Fig. 8e). For PS films with no Hb adsorbed, the peak for direct reduction of oxygen was observed at about −0.8 V (Fig. 8b), at least 0.4 V more negative than the potential of the catalytic peak. The catalytic efficiency expressed as the ratio of reduction peak current of HbFe(III) in the presence (I_c) and absence (I_d) of oxygen, I_c/I_d, decreased with an increase of scan rate (Fig. 9), also characteristic of electrochemical catalytic reduction [42]. With the lower scan rate, the catalytic reaction cycle with a fixed reaction rate would have more time to repeat, leading to a higher number of catalytic cycles. Thus, compared with the faster scan rate, the lower scan rate would increase the ratio of I_c/I_d. For Hb-PS film system, the catalytic efficiency at 0.2 V s^{-1} for oxygen (6.0) is much larger than that of Hb-PAMAM (3.6) [43] and Hb-CS (4.6) [14] films at the same scan rate, indicating that this new kind of protein films may have a potential perspective in electrochemical catalysis and biosensing.

The mechanism of electrocatalytic reduction of oxygen at Mb-DDAB film electrodes was studied previously [44]. The electrochemical reduction of MbFe(III) to MbFe(II) in DDAB films occurred at the electrode, followed by a fast reaction of MbFe(II) with oxygen, forming MbFe(II)-O_2. This chemical reaction product then underwent electrochemical reduction at the potential of MbFe(III) reduction, produced hydrogen peroxide and MbFe(II) again, thus forming a catalytic cycle. Although the mechanistic issue concerning catalytic reduction of O_2 at Hb-PS film electrodes is beyond the scope of the current work, we believe that it would be similar to that for Mb-DDAB films.

The catalytic activity of the Hb-PS films toward hydrogen peroxide was also investigated. Compared with the CV in the absence of H_2O_2 at a pH 7.0 buffer (Fig. 10c), an obvious increase in the reduction peak at about −0.4 V was observed after H_2O_2 was added (Fig. 10d). The increase of reduction peak current was accompanied by the disappearance of the oxidation peak. The reduction peak current increased with the concentration of H_2O_2 in solution (Fig. 10e). However, direct reduction of H_2O_2 at blank PS film electrodes was not observed (Fig. 10b). The catalytic reduction of H_2O_2 at Hb-PS film electrodes could be used to determine H_2O_2 concentration in solution by CV. The reduction peak had a linear relationship with H_2O_2 concentration in the range of 6.6–130 μM with a detection limit of 2 μM.

At Hb-PS film electrodes, the position of catalytic reduction peak potential of hydrogen peroxide was almost the same as that of oxygen (Figs. 8 and 10), indicating the similarity of the reaction mechanism

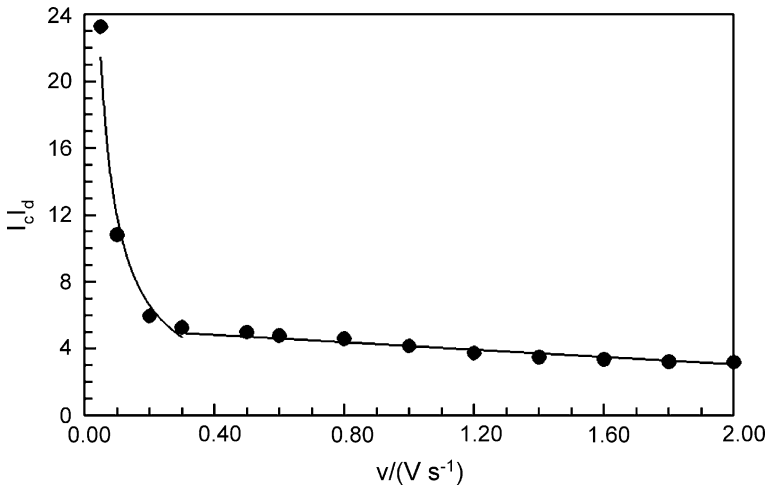

Fig. 9. Influence of scan rate on catalytic efficiency, I_c/I_d, for Hb-PS film electrode in 10 ml of pH 7.0 buffer solutions, where I_c is the CV reduction peak current in buffers with 60 ml of air injected and I_d is the CV reduction peak current in buffer without oxygen.

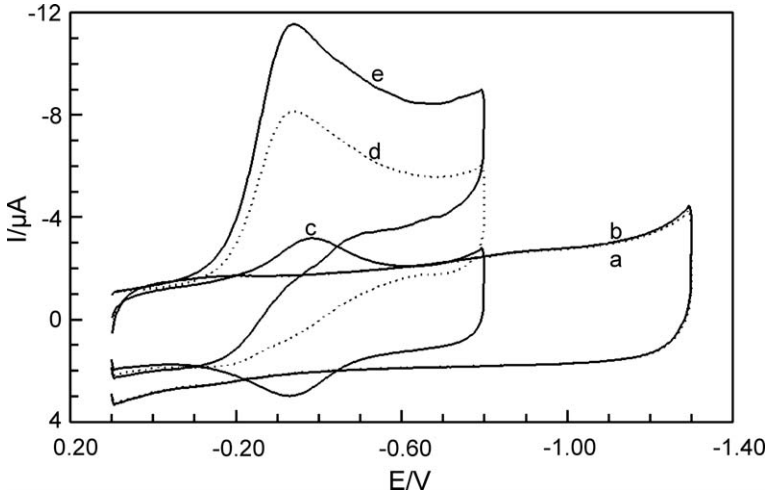

Fig. 10. Cyclic voltammograms at 0.2 V s^{-1} in pH 7.0 buffers for (a) PS films with no H_2O_2 present, (b) PS films with 0.025 mM H_2O_2 present, (c) Hb-PS films with no H_2O_2 present, (d) Hb-PS films with 0.005 mM H_2O_2 present, (e) Hb-PS films with 0.025 mM H_2O_2 present.

between the two systems. The exact mechanism of catalytic reduction of hydrogen peroxide on Hb-PS films is not yet clear and beyond the scope of the present study. However, it is probably similar to that of horseradish peroxide-Eastman AQ (HRP-AQ) film system [45], since Hb and HRP are all heme proteins and have similar electrochemical properties. In HRP-AQ film system, the oxidation product of HbFe(III) by H_2O_2 could be also reduced by H_2O_2, and producing native HbFe(III) again and O_2. It is the production of O_2 that makes the electrocatalytic CV behavior of H_2O_2 similar to that of O_2 at HRP-AQ film electrodes.

4. Conclusions

The positively charged hemoglobin at pH 5.0 can be adsorbed on the negatively charged surface of polystyrene latex beads mainly by electrostatic attraction between them. Hb retains its near native structure in Hb-PS films in its dry form and in the medium pH range. The procedure of adsorption/washing steps in the assembly of Hb-PS particles acts like a purification process and removes the impurities existing in Hb solution. This may greatly contribute to the good electroactivity of Hb in PS films. The stable Hb-PS films also demonstrate good electrocatalytic properties toward different substrates of environmental or biological significance. This novel approach that combines the assembly of protein shells on colloid particles with the fabrication of protein-coated particle films on electrodes may provide a new promising method to realize the direct electrochemistry of proteins. This kind of protein films may also provide a perspective possibility as the new type of biosensors based on direct or mediator-free electrochemistry of proteins.

Acknowledgements

The financial support of the National Natural Science Foundation of China (NSFC 29975003 and 20275006) is gratefully acknowledged.

References

[1] Y. Lvov, H. Mohwald (Eds.), Protein Architecture: Interfacing Molecular Assemblies and Immobilization Biotechnology, Marcel Dekker, New York, 2000, pp. 1–394.
[2] T.A. Horbett, J.L. Brash (Eds.), Protein at Interfaces: Fundamentals and Applications, ACS Symposium Series, vol. 602, American Chemical Society, Washington DC, 1995, pp. 1–79.
[3] A.P.F. Turner, I. Karube, G.S. Wilson (Eds.), Biosensors: Fundamentals and Applications, Oxford Univ. Press, Oxford, 1987, pp. 1–770.
[4] J.F. Rusling, Z. Zhang, Thin films on electrodes for direct protein electron transfer, in: R.W. Nalwa (Ed.), Handbook of Surfaces and Interfaces of Materials, vol. 5, Academic Press, New York, 2001, pp. 33–71.

[5] N. Hu, Direct electrochemistry of redox proteins or enzymes at various film electrodes and their possible applications in monitoring some pollutants, Pure Appl. Chem. 73 (2001) 1979–1991.
[6] F.A. Armstrong, H.A.O. Hill, N.J. Walton, Direct electrochemistry of redox proteins, Acc. Chem. Res. 21 (1988) 407–413.
[7] M.F. Chaplin, C. Bucke, Enzyme Technology, Cambridge Univ. Press, Cambridge, UK, 1990.
[8] L. Gorton, A. Lindgren, T. Larsson, F.D. Munteanu, T. Ruzgas, I. Gazaryan, Direct electron transfer between heme-containing enzymes and electrodes as basis for third generation biosensors, Anal. Chim. Acta 400 (1999) 91–108.
[9] A.-E.F. Nassar, Z. Zhang, N. Hu, J.F. Rusling, T.F. Kumosinski, Proton-coupled electron transfer from electrodes to myoglobin in ordered biomembrane-like films, J. Phys. Chem., B 101 (1997) 2224–2231.
[10] J. Yang, N. Hu, Direct electron transfer for hemoglobin in biomembrane-like dimyristoyl phosphatidylcholine films on pyrolytic graphite electrodes, Bioelectrochem. Bioenergy 48 (1999) 117–127.
[11] N. Hu, J.F. Rusling, Electrochemistry and catalysis with myoglobin in hydrated poly(ester sulfonic acid) ionomer films, Langmuir 13 (1997) 4119–4125.
[12] H. Sun, N. Hu, H. Ma, Direct electrochemistry of hemoglobin in polyacrylamide hydrogel films on pyrolytic graphite electrodes, Electroanalysis 12 (2000) 1064–1070.
[13] H. Lu, Z. Li, N. Hu, Direct voltammetry and electrocatalytic properties of catalase incorporated in polyacrylamide hydrogel films, Biophys. Chemist. 104 (2003) 623–632.
[14] H. Huang, N. Hu, Y. Zeng, G. Zhou, Electrochemistry and electrocatalysis with heme proteins in chitosan biopolymer films, Anal. Biochem. 308 (2002) 141–151.
[15] H. Liu, N. Hu, Heme protein-gluten films: voltammetric studies and their electrocatalytic properties, Anal. Chim. Acta 481 (2003) 91–99.
[16] Y. Zhou, N. Hu, Y. Zeng, J.F. Rusling, Heme protein-clay films: direct electrochemistry and electrochemical catalysis, Langmuir 18 (2002) 211–219.
[17] D. Cao, P. He, N. Hu, Electrochemical biosensors utilizing electron transfer in heme proteins immobilized on Fe_3O_4 nanoparticles, Analyst 128 (2003) 1268–1274.
[18] H. Sun, H. Ma, N. Hu, Electroactive hemoglobin–surfactant–polymer biomembrane-like films, Bioelectrochem. Bioenergy 49 (1999) 1–10.
[19] L. Wang, N. Hu, Electrochemistry and electrocatalysis with myoglobin in biomembrane-like DHP–PDDA polyelectrolyte–surfactant complex films, J. Colloid Interface Sci. 236 (2001) 166–172.
[20] X. Chen, N. Hu, Y. Zeng, J.F. Rusling, J. Yang, Ordered electrochemically-active films of hemoglobin, didodecyldimethylammonium ions and clay, Langmuir 15 (1999) 7022–7030.
[21] H. Ma, N. Hu, J.F. Rusling, Electroactive myoglobin films grown layer-by-layer with poly(styrenesulfonate) on pyrolytic graphite electrodes, Langmuir 16 (2000) 4969–4975.
[22] P. He, N. Hu, G. Zhou, Assembly of electroactive layer-by-layer films of hemoglobin and polycationic poly(diallyldimethyl ammonium), Biomacromolecules 3 (2002) 139–146.
[23] Y. Zhou, Z. Li, N. Hu, Y. Zeng, J.F. Rusling, Layer-by-layer assembly of ultrathin films of hemoglobin and clay nanoparticles with electrochemical and catalytic activity, Langmuir 18 (2002) 8573–8579.
[24] Z. Li, N. Hu, Direct electrochemistry of heme proteins in their layer-by-layer films with clay nanoparticles, J. Electroanal. Chem. 558 (2003) 155–165.
[25] F. Caruso, H. Mohwald, Protein multilayer formation on colloids through a stepwise self-assembly technique, J. Am. Chem. Soc. 121 (1999) 6039–6046.
[26] F. Caruso, C. Schuler, Enzyme multilayers on colloid particles: assembly, stability, and enzymatic activity, Langmuir 16 (2000) 9595–9603.
[27] Y. Lvov, F. Caruso, Biocolloids with ordered urease multilayer shells as enzymatic reactors, Anal. Chem. 73 (2001) 4212–4217.
[28] C. Schuler, F. Caruso, Preparation of enzyme multilayers on colloids for biocatalysis, Macromol. Rapid Commun. 21 (2000) 750–753.
[29] J.B. Matthew, G.I.H. Hanania, F.R.N. Gurd, Electrostatic effects in hemoglobin–hydrogen–ion equilibria in human deoxyhemoglobin and oxyhemoglobin-A, Biochemistry 18 (1979) 1919–1928.
[30] H. Theorell, A. Ehrenberg, Spectrophotometric, magnetic, and titrimetric studies on the heme-linked groups in myoglobin, Acta Chem. Scand. 5 (1951) 823–848.
[31] P. George, G.I.H. Hanania, Spectrophotometric study of ionizations in methemoglobin, Biochem. J. 55 (1953) 236–243.
[32] Q. Huang, Z. Lu, J.F. Rusling, Composite films of surfactants, Nafion, and proteins with electrochemical and enzyme activity, Langmuir 12 (1996) 5472–5480.
[33] A-E.F. Nassar, W.S. Willis, J.F. Rusling, Electron transfer from electrodes to myoglobin: facilitated in surfactant films and blocked by adsorbed biomacromolecules, Anal. Chem. 67 (1995) 2386–2392.
[34] R.W. Murray, Chemically Modified Electrodes, in: A.J. Bard (Ed.), Electroanalytical Chemistry, vol. 13, Marcel Dekker, New York, 1986, pp. 191–368.
[35] A.M. Bond, Modern Polarographic Methods in Analytical Chemistry, Marcel Dekker, New York, 1980.
[36] A.-S. Yang, B. Honig, Structural origins of pH and ionic strength effects on protein stability. Acid denaturation of sperm whale apomyoglobin, J. Mol. Biol. 237 (1994) 602–614.
[37] D. Bashford, D.A. Case, C. Dalvit, L. Tennant, P.E. Wright, Electrostatic calculations of side-chain pK_a values in myoglobin and comparison with NMR data for histidines, Biochemistry 32 (1993) 8045–8056.
[38] J.J. O'Dea, J.G. Osteryoung, Characterization of quasi-reversible surface processes by square-wave voltammetry, Anal. Chem. 65 (1993) 3090–3097.
[39] Z. Zhang, J.F. Rusling, Electron transfer between myoglobin and electrodes in thin films of phosphatidylcholines and dehexadecylphosphate, Biophys. Chem. 63 (1997) 133–146.

[40] F. Rusling, Enzyme bioelectrochemistry in cast biomembrane-like films, Acc. Chem. Res. 31 (1998) 363–369.
[41] A.-E.F. Nassar, J.M. Bobbitt, J.O. Stuart, J.F. Rusling, Catalytic reduction of organohalide pollutants by myoglobin in a biomembrane-like surfactant film, J. Am. Chem. Soc. 117 (1995) 10986–10993.
[42] C.P. Andrieux, C. Blocman, J.-M. Dumas-Bouchiant, F. M'Halla, J.M. Saveant, Homogeneous redox catalysis of electrochemical reactions: Part V. Cyclic voltammetry, J. Electroanal. Chem. 113 (1980) 19–40.
[43] L. Shen, N. Hu, Heme-protein films with polyamidoamine dendrimer: direct electrochemistry and electrocatalysis, Biochim. Biophys. Acta, Bioenerg. 1608 (2004) 23–33.
[44] A.C. Onuoha, J.F. Rusling, Electroactive myoglobin–surfactant films in a bicontinuous microemulsion, Langmuir 11 (1995) 3296–3301.
[45] R. Huang, N. Hu, Direct electrochemistry and electrocatalysis with horseradish peroxidase in Eastman AQ films, Bioelectrochemistry 54 (2001) 75–81.